

## Stress Relaxation in Molten Polymers. IV

C. MUSSA, P. SACERDOTE, P. GUGLIELMINO, and V. TABLINO,  
*Montecatini S.p.A. and Istituto Chimico dell'Università,  
 Torino, Italy*

### Synopsis

After a survey of suggested analytical methods, data are given for ten polymer samples (high and low pressure polyethylenes, atactic and isotactic polypropylenes, and of natural rubbers). It appears that the suggested methods of plotting the stress relaxation data after cessation of steady flow, as well as the quantities defined from such analysis, in the case of the given polymers can yield qualitative and semiquantitative information on such structural features such as average chain length, polydispersity, chain regularity, long branching, and crosslinking.

In previous work<sup>1-3</sup> a general procedure was suggested, starting from the following working hypotheses.

(1) The stress relaxation phenomenon can be described by means of unidimensional equations. Some experimental facts, as the Weissenberg effect, make us doubt the reliability of this assumption. Nevertheless, since our aim was to establish a set of simple equations enabling us to get at an approximate quantitative evaluation of stress relaxation following viscous flow, we will adopt the unidimensional scheme, which is common to most practical rheological calculations.

(2) A general equation of the Maxwell type is assumed as fundamental:

$$\mathfrak{T} = -\eta(d\gamma/dt) \quad (1)$$

In general, the viscosity factor  $\eta$  must be considered as a function of the relaxation stress  $\mathfrak{T}$ , of the time, and possibly also of other variables.

(3) It is assumed that

$$d\gamma/dt = (d\gamma/d\mathfrak{T})(d\mathfrak{T}/dt) \quad (2)$$

i.e., that the strain  $\gamma$  (a number, namely a ratio between displacement and length) is a function of time only through the time-dependent variable stress. This assumption enables us to introduce the function  $d\gamma/d\mathfrak{T}$ , the "elasticity factor" or "elasticity law," a factor describing the kind of elasticity concerned in this phenomenon. This function has the dimensions of a compliance.

It must be stressed once more that the strain considered here must not be confused with the strain considered in the viscous flow or in any other

phenomenon where an actual displacement or deformation is measured. The strain considered here is a purely theoretical, nonmeasurable strain associated with the relaxation phenomenon, in order to establish eq. (1), which sets the problem according to the viscoelastic scheme. The real strains acting in the relaxation phenomenon are the wriggling motions of the macromolecules stretched during viscous flow and the change in their configurations when the material relaxes after cessation of the viscous flow. The strain considered here can be thought of as some statistical average of such motions. Rheological measurements are not expected to be sufficient to give us any parameter related to such strains. Perhaps experiments of stress or flow birefringence can be used in this connection.

By combining eqs. (1) and (2), by multiplying by  $t$  and dividing by  $\mathfrak{C}$  we obtain:

$$t = Rn \quad (3)$$

where

$$R = \eta(d\gamma/d\mathfrak{C}) \quad (4)$$

and

$$n = -d \log \mathfrak{C} / d \log t \quad (5)$$

The following points must be stressed: The multiplication by  $t$  and the division by  $\mathfrak{C}$  are always possible except on the straight lines  $t = 0$  and  $\mathfrak{C} = 0$ . Such lines of variability correspond to very short or very long times. Hence, eq. (3) is valid in the whole practical field of our actual measurements.

The function  $R$  defined by eq. (4) is dimensionally a time. When the relaxing system is a Maxwell (or a Voigt) body, this function becomes a constant where the classical relaxation (or retardation) time of the body is considered. It was suggested<sup>3</sup> that the  $R$  values be assumed as relaxation times associated with any one of the corresponding values of the relaxing stress. A kind of relaxation spectrum is obtained in this way.

We want to emphasize that when the new characteristic function  $R$  is so defined, the elastic factors are not separated from the viscous ones. It is likely that a theory avoiding such an arbitrary partition has some theoretical advantages. The numerical function  $n$  defined by eq. (5) is a direct and convenient result of the experimental determinations since the wide range of stresses and times considered makes it necessary to use a log-log plot. Furthermore, such a plot allows a more correct consideration of the relative uncertainties. The only drawback is that graphic differentiation means summing up the uncertainties of both parameters. A careful consideration of such uncertainties must always be made in order to know the limits of availability of the above defined function  $R$ .

From eqs. (3) and (4) we obtain

$$R = \eta(d\gamma/d\mathfrak{C}) = t/n \quad (6)$$

The analytical procedure resulting from eq. (6) is the following.

From the experimental plots of the data giving  $\log \mathfrak{T}$  as a function of  $\log t$  the value of  $n$  is calculated by graphic derivation. By means of eqs. (5) and (6) it is possible to plot the graphs of  $\mathfrak{T}$  as a function of  $R$ . As usual, log-log plots must be preferred.

If the working hypotheses are correct, for a given polymer at a given temperature, a unique  $\log \mathfrak{T}$  versus  $\log R$  plot independent of the initial stress is expected. Indeed, from the phenomenon of the relaxation isochronism it is to be expected that such condition is automatically fulfilled in the whole isochronic region (in most cases, the widest part of the recorded relaxation curve).

The use of such plot as a fingerprint of a polymer, giving us such information on the long-range structural features, as chain length, polydispersity, average chain irregularities, long-chain branching, crosslinks is suggested.

Otherwise, we can match the experimental data with some particular analytical law

$$F(\mathfrak{T}) = \eta(d\gamma/d\mathfrak{T}) \quad (7)$$

suggested by theoretical considerations. In this last connection, the following procedure can be used: the given analytical function  $F(\mathfrak{T})$  is substituted in eqs. (1) and (2). We obtain:

$$-dt = [F(\mathfrak{T})/\mathfrak{T}]d\mathfrak{T} = F(\mathfrak{T})d(\log \mathfrak{T}) \quad (8)$$

By integration, a law  $t = f(\mathfrak{T})$  is obtained, which can be matched with the experimental  $t = f(\mathfrak{T})$  curve. This procedure, which has already been followed in a previous study,<sup>2</sup> can be termed the procedure of integral straight line plots.

When integration is not convenient, a differential procedure is also available, namely the procedure of differential straight line plots. From eq. (6) we obtain:

$$\log R = \log (t/n) = \log F(\mathfrak{T}) \quad (9)$$

The values of  $\log R$  corresponding to any measured values of  $\mathfrak{T}$  are known from the experimental data and are plotted as abscissas. By means of a trial-and-error procedure or by means of tabulated values of the suggested function  $F(\mathfrak{T})$  (which is ordinarily a function of  $\mathfrak{T}$  and of some parameters dependent on the polymer structure) the values of  $\log F(\mathfrak{T})$  are plotted in the ordinates. The plot giving the better straight line with a 45° slope does define the wanted structural parameters. Some other experimental features can help us in this choice: e.g., the values of the relaxation areas or the (approximately constant) value of the time lag  $\Delta t$  between two curves corresponding to two different (possibly high) initial values  $\mathfrak{T}_{ss}$  of the relaxing stress.

Some experimental instances are reported now in order to check how these analytical methods can be practically used.

TABLE I

Sample	Polymer	Intrinsic viscosity, dl./g.	Newtonian melt viscosity, (poises $\times 10^{-4}$ )	Tempera- ture, °C.	$\tau_{\text{res}} \times 10^{-3}$ at various rates of shear, dynes/cm. <sup>2</sup>					Elasticity number
					2.7 sec. <sup>-1</sup>	0.9 sec. <sup>-1</sup>	0.27 sec. <sup>-1</sup>	0.027 sec. <sup>-1</sup>	0.027 sec. <sup>-1</sup>	
A	Polypropylene (atactic)	0.80	1.5	160	11	4	0.41	0.57	0.40	
				180	7	2.1	0.24	0.40		
B	Polypropylene (isotactic)	0.90	0.56	200	4.5	1.5	0.17	0.26	1.15	
				160	3.9	1.5		0.75		
C	Polypropylene ( $\bar{M}_w/\bar{M}_n \approx 4$ )	0.95	0.38	200	2.6	0.9		0.70	0.90	
				160	4.6	0.6		0.70		
D	Polypropylene ( $\bar{M}_w/\bar{M}_n \approx 20$ )	1.07	1.00	160	22.6	2.8		0.90	0.70	
				200	15.5	1.8		0.60		
E	Polyethylene (low pressure)	1.30	2.5	160	10	1.1		0.7	1.05	
				180	17	4.9		0.4		
			1.0	200	13	2.1	0.3	0.90	0.90	
			15	160	43	20	3.4	2.7	1.08	
			12	180	36	16	2.7	0.75	0.75	
			10	200	31	12.5	2.2	0.52	0.52	



### Experimental

We will report here the data for ten samples, of which four are the same considered previously;<sup>2,4</sup> four of the others are polypropylenes, namely an atactic and an isotactic one having similar intrinsic viscosities and two isotactic polypropylenes of widely different polydispersity and similar chain length; the remaining two samples were cut from a natural rubber, one being unvulcanized and one submitted to slight curing. In Table I the known features of all samples are summarized, together with the experimental conditions (temperatures, rates of shear of the viscous flow preceding the stress relaxation, corresponding initial stresses  $\mathfrak{T}_{ss}$ ). The stresses were measured by means of a Kepes consistometer. The relaxation times were recorded by means of a hand chronometer. Relaxation times of less than 1 sec. must be considered as approximate at  $\pm 0.1$  sec. Thus, the investigation of the shortest relaxation times in our experimental conditions is only approximate. A special experimental device must be planned in order to investigate this important field of variability. The temperatures were kept constant at  $\pm 0.1^\circ\text{C}$ . and the specimens were kept under a steady current of  $\text{N}_2$  during the whole investigation time.

### Results

We will consider first, as an example, specimen E (low pressure polyethylene having an intrinsic viscosity of 1.30 dl./g.). In Table II experimental relaxation data for this polymer are given, namely: for each value of  $\gamma$ , at each temperature, in the first and second columns are given the stresses  $\mathfrak{T}$  and their logarithms, in the third and fourth columns are listed the corresponding times  $t$  and their logarithms, in the fifth and sixth columns are given the derivatives  $n = -d \log \mathfrak{T} / d \log t$  and their logarithms; the seventh column lists values of  $\log t/n = \log R$ .

Such data are given for three temperatures (160, 180, and  $200^\circ\text{C}$ .) and, at each temperature, three elementary experimental runs are made, corresponding to three different initial stresses.

For the two lowest  $\mathfrak{T}_{ss}$  we give (in the eighth column) the differences  $\Delta t$  (corresponding to any measured stress value) between the relaxation time of the curve starting from the given lower  $\mathfrak{T}_{ss}$  and the one of the curve starting from the highest  $\mathfrak{T}_{ss}$ . An estimated average value  $(\Delta t)_{av}$  is also given, corresponding to the intermediate part of the relaxation curves, where the time lag  $\Delta t$  can better be evaluated and where it appears to be approximately constant.<sup>2,3</sup>

The primary (experimental) relaxation graphs are given (as  $\log \mathfrak{T}$  versus  $\log t$  plots) in Figure 1 for  $180^\circ\text{C}$ . From such graphs the values of  $n = -d \log \mathfrak{T} / d \log t$  are graphically calculated.

Figure 2 is the graph of  $\log \mathfrak{T}$  versus  $\log R$ ; such graphs are called here normalized stress relaxation graphs. It is seen from Figure 2 that with increasing initial stresses such graphs tend actually to overlap in a unique graph (within the limits of reproductibility and of experimental accuracy).

TABLE II  
Data for Sample E

T, °C.	$\dot{\gamma} = 0.9 \text{ sec.}^{-1}$					$\dot{\gamma} = 0.27 \text{ sec.}^{-1}$					$\dot{\gamma} = 0.027 \text{ sec.}^{-1}$				
	$\frac{\mathcal{P}}{\text{dynes/cm.}^2}$	$\log \frac{\mathcal{P}}{\text{dynes/cm.}^2}$	t, sec.	$\log t$	$\log \frac{t}{n}$	$\frac{\mathcal{P}}{\text{dynes/cm.}^2}$	$\log \frac{\mathcal{P}}{\text{dynes/cm.}^2}$	t, sec.	$\log t$	$\log \frac{t}{n}$	$\frac{\mathcal{P}}{\text{dynes/cm.}^2}$	$\log \frac{\mathcal{P}}{\text{dynes/cm.}^2}$	t, sec.	$\log t$	$\log \frac{t}{n}$
160	8570	3.93	0.9	1.95	0.49	8570	3.93	0.6	1.78	0.49	1720	3.24	6	0.78	0.56
	4310	3.63	3.5	0.54	0.64	4310	3.63	2.6	0.41	0.54	855	2.93	20	1.30	0.63
	1720	3.24	13	1.11	0.80	1720	3.24	12	1.08	0.72	380	2.58	62	1.79	0.90
	855	2.93	28	1.45	0.89	855	2.93	28	1.45	0.89	190	2.28	135	2.13	0.98
	380	2.58	59	1.77	0.89	380	2.58	132	2.12	0.98	94.5	1.97	276	2.44	0.98
	190	2.28	128	2.11	0.97	190	2.28	270	2.43	0.98	$\mathcal{P}_{ss} = 43,000$			$\mathcal{P}_{ss} = 3,400$	
180	8570	3.93	0.6	1.78	0.57	8570	3.93	0.4	1.60	0.48	1720	3.24	2	0.30	0.40
	4310	3.63	2	0.30	0.63	4310	3.63	1.6	0.20	0.55	855	2.93	10	1.00	0.55
	1720	3.24	8	0.90	0.75	1720	3.24	7.6	0.88	0.65	380	2.58	35	1.54	0.86
	855	2.93	19	1.28	0.91	855	2.93	18.6	1.27	0.87	190	2.28	71	1.85	1.02
	380	2.58	40	1.60	1.03	380	2.58	42	1.61	1.03	94.5	1.97	138	2.14	1.05
	190	2.28	70	1.84	1.05	190	2.28	135	2.13	1.06	$\mathcal{P}_{ss} = 36,000$			$\mathcal{P}_{ss} = 2,700$	
200	8570	3.93	0.5	1.70	0.72	8570	3.93	0.3	1.48	0.58	1720	3.24	0.8	0.8	0.32
	4310	3.63	1.2	0.68	0.72	4310	3.63	1	0	0.62	855	2.93	6	0.78	0.57
	1720	3.24	4.6	1.28	0.76	1720	3.24	4.5	1.02	0.91	380	2.58	21	1.33	1.04
	855	2.93	10	1.00	0.89	855	2.93	23	1.36	1.10	190	2.28	40	1.60	1.15
	380	2.58	22	1.34	1.08	380	2.58	40	1.60	1.18	94.5	1.97	71	1.85	1.23
	190	2.28	39	1.59	1.18	190	2.28	72	1.86	1.28	$\mathcal{P}_{ss} = 31,000$			$\mathcal{P}_{ss} = 2,200$	

We will assume the "true" normalized stress relaxation graphs to be those obtained from the highest  $\bar{\mathcal{T}}_{ss}$  value used in our experiments. It can be noticed that, in order to obtain the normalized stress relaxation graph, it is necessary to operate at the highest  $\bar{\mathcal{T}}_{ss}$  values which can be reached in the

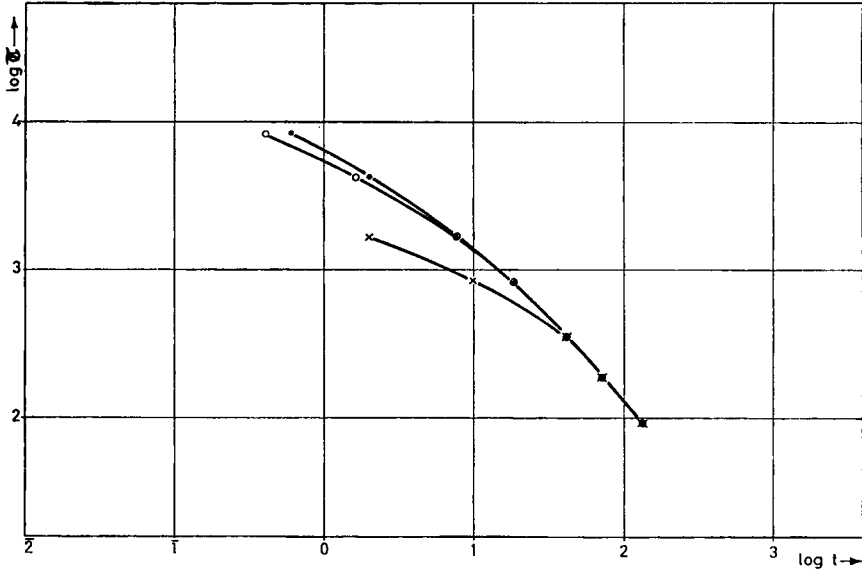


Fig. 1. Experimental relaxation graphs for sample E at 180°C.: (●)  $\bar{\mathcal{T}}_{ss} = 36,000$ ; (○)  $\bar{\mathcal{T}}_{ss} = 16,000$ ; (×)  $\bar{\mathcal{T}}_{ss} = 2,700$ .

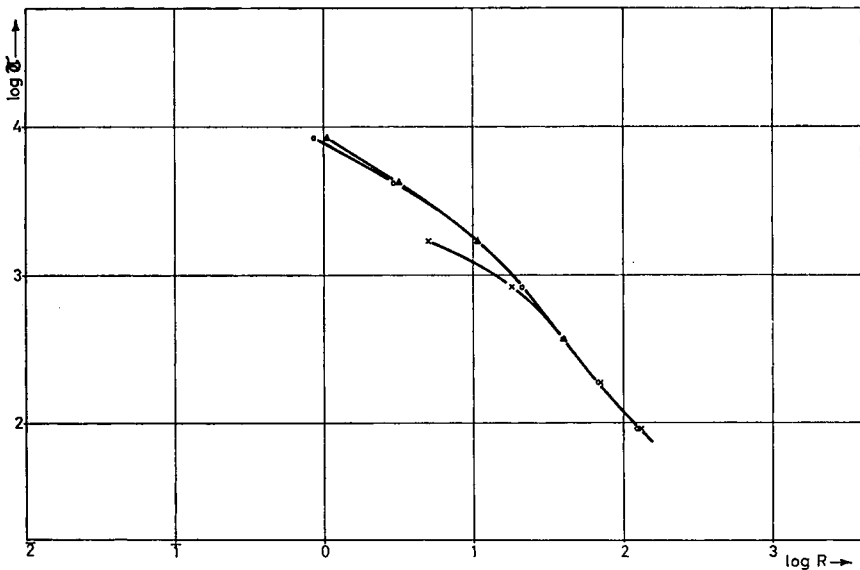


Fig. 2. Normalized stress relaxation graphs for sample E at 180°C.: (▲)  $\bar{\mathcal{T}}_{ss} = 36,000$ ; (○)  $\bar{\mathcal{T}}_{ss} = 16,000$ ; (×)  $\bar{\mathcal{T}}_{ss} = 2,700$ .



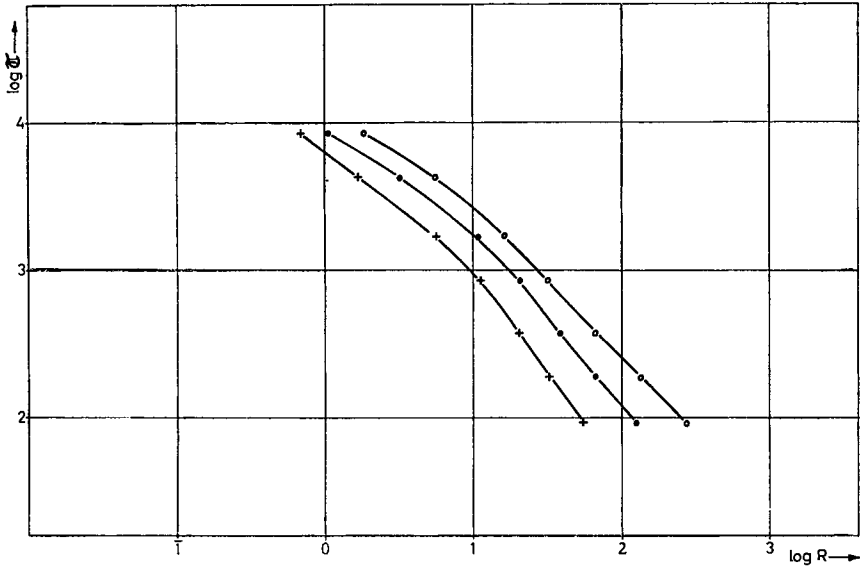


Fig. 3. Normalized stress relaxation graphs for sample E at various temperatures: (O)  $T = 160^{\circ}\text{C.}$ ; (●)  $T = 180^{\circ}\text{C.}$ ; (+)  $T = 200^{\circ}\text{C.}$

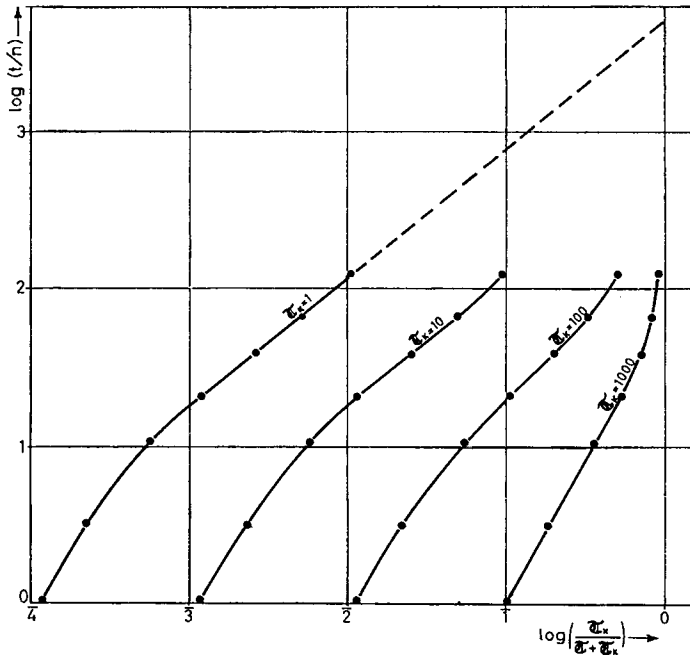


Fig. 4. Differential straight line plots for sample E at  $180^{\circ}\text{C.}$  for various values of  $\tau_x$  and  $\tau_{ss} = 36,000$ .

given experimental conditions. In Figure 3 the three normalized stress relaxation graphs corresponding to the different temperatures are plotted. Such sets of graphs can be taken as a basis for investigating a possible extension of the principle of the corresponding states to the cases of nonlinear systems. Figure 4 is an illustration of the method of the differential straight line plots, assuming we are dealing with a viscoelasticity of the parabolic type:

$$F(\mathfrak{T}) = \lambda_K [\mathfrak{T}_K / (\mathfrak{T} + \mathfrak{T}_K)]^\alpha \quad (10)$$

When eq. (8) is integrated, we have:

$$C - t = \int [F(\mathfrak{T})/\mathfrak{T}] d\mathfrak{T} \quad (11)$$

The integration constant  $C$  is determined by the boundary condition:  $\mathfrak{T} = \mathfrak{T}_{ss}$  at  $t = 0$ . When

$$\Phi(\mathfrak{T}) = \int [F(\mathfrak{T})/\mathfrak{T}] d\mathfrak{T}$$

it will be:

$$C = \Phi(\mathfrak{T}_{ss}) \quad (12)$$

Substituting eq. (10) in eq. (12), we can assume (for  $\mathfrak{T}_{ss} \gg \mathfrak{T}_K$ ) the following approximative formula

$$C = -\lambda_K \mathfrak{T}_K^\alpha / \alpha \mathfrak{T}_{ss}^\alpha$$

Then, the time lag  $\Delta t$  between two relaxation curves starting from two different initial stresses  $\mathfrak{T}_{ss}^I$  and  $\mathfrak{T}_{ss}^{II}$  will be

$$\Delta t = (\lambda_K \mathfrak{T}_K^\alpha / \alpha) [(1/\mathfrak{T}_{ss}^{II})^\alpha - (1/\mathfrak{T}_{ss}^I)^\alpha] \quad (13)$$

It is seen from Figure 4 that the parameter  $\mathfrak{T}_K$  is poorly defined: no plot is truly linear, and many plots are only approximately linear. We can choose the more linear plot defining those  $\lambda_K$  and  $\mathfrak{T}_K$  values which better fulfill the condition expressed by eq. (13).

It is stressed that the abscissa:  $\log [\mathfrak{T}_K / (\mathfrak{T} + \mathfrak{T}_K)]$  is defined between  $-\infty$  and 0 and that the  $\lambda_K$  is given by the intercept of the straight line differential graph (when it exists) with the straight line:  $\log [\mathfrak{T}_K / (\mathfrak{T} + \mathfrak{T}_K)] = 0$ , while the slope of the same graph gives the exponent  $\alpha$ . In the given case, the above considerations yield the following values:  $\alpha = 0.85 \pm 0.02$ ;  $\mathfrak{T}_K = \sim 1$ ;  $\lambda_K = \sim 5000$ .

Figure 5 shows the normalized stress relaxation graphs of samples A, B, C, and D at 180°C; Figure 6 shows those of samples E, F, G, H, I, and L at the same temperature. In Table III are given the values of the parameters of parabolic elasticity ( $\alpha$ ,  $\mathfrak{T}_K$ ,  $\lambda_K$ ) for the few instances where it was possible to define them with sufficiently good accuracy, by means of the differential straight line plots.

In Figure 7 are represented the normalized stress relaxation graphs for samples A and B (atactic and isotactic polypropylene) at three different temperatures. It is noteworthy that the plot of the isotactic sample at

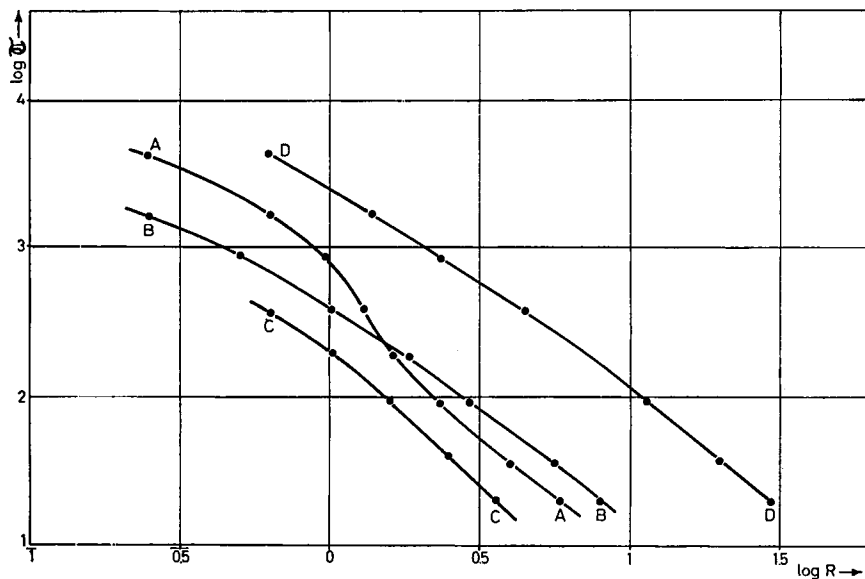


Fig. 5. Normalized stress relaxation graphs at 180°C. for samples A, B, C, and D.

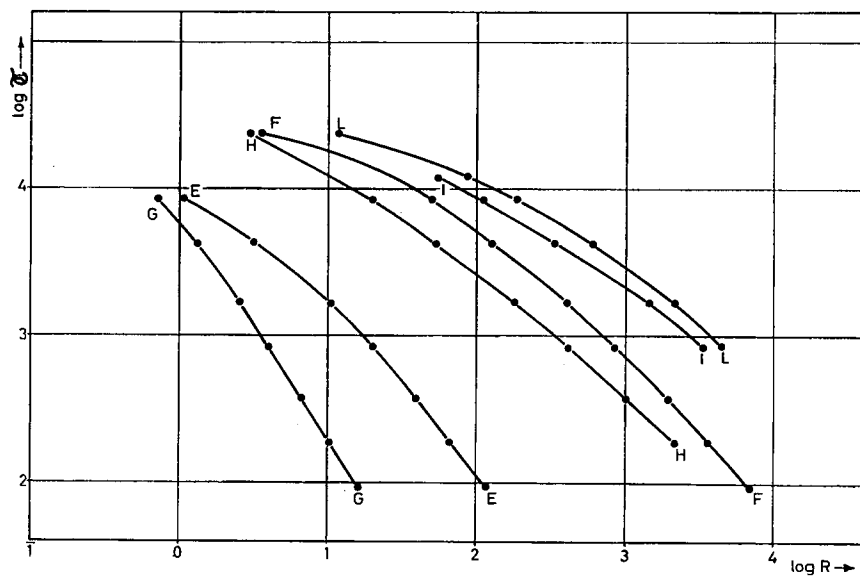


Fig. 6. Normalized stress relaxation graphs at 180°C. for samples E, F, G, H, I, and L.

160°C. (i.e., below its melting point) is more shifted towards the left than the plot at 180°C. as compared with the one at 200°C., the shifting being higher at longer relaxation times  $R$ . On the contrary, the normalized stress relaxation graphs for atactic polypropylene at the three different tempera-

tures are nearly equally spaced (c.f. polyethylene above the melting point, Sample E in Fig. 3). Furthermore, for isotactic polypropylenes, the increase in the elastic number when the temperature goes from 180 to 160°C. is greater than the increase noticed when the temperature decreases from

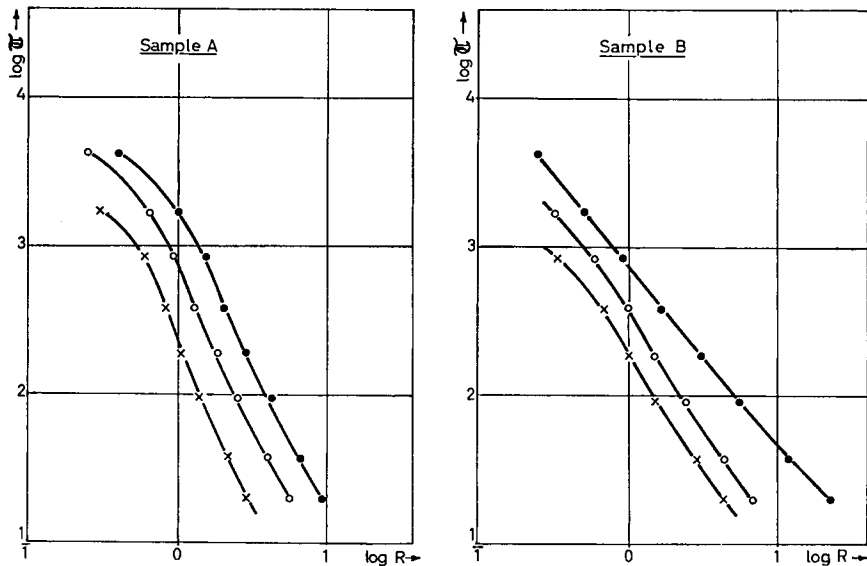


Fig. 7. Normalized stress relaxation graphs for samples A and B at various temperatures: (●)  $T = 160^{\circ}\text{C.}$ ; (○)  $T = 180^{\circ}\text{C.}$ ; (×)  $T = 200^{\circ}\text{C.}$

200 to 180°C. (see Table I). These phenomena are attributed to crystallization taking place during the long lasting relaxation. Thus, in this connection, the influence of crystallization is analogous to the influence of crosslinks, as it will be seen below.

### Discussion

Figures 5 and 6 show that: when the other structural features (chain regularity, polydispersity, crosslinking and long-branching) are equal, an increase of the average chain length (as defined by the intrinsic viscosity) brings about a displacement of the normalized stress relaxation curves from left to right, namely, towards higher  $R$ .

Further, for nearly equal chain lengths a higher irregularity of the chain brings about highest values of the relaxation stresses corresponding to the lowest relaxation times  $R$ , namely a steeper normalized stress relaxation graph.

Also a higher polydispersity brings about a shift of the whole normalized stress relaxation curve towards higher  $R$ . This shift is not wholly parallel (being somewhat larger for the lowest stresses). The effect of polydispersity is similar to that of an increase of the average molecular weight.

TABLE III  
Parameters of parabolic elasticity at 180°C.

Sample	Intrinsic viscosity, dl./g.	$\tau_K$	$\alpha$	$\lambda_K$	Linearity range of stresses
A	0.80	1	0.50	28	20-1,700
B	0.90	1	0.62	53	20-400
C	0.95	(1)	(0.70)	(23)	(20-100)
D	1.07	—	—	—	—
E	1.30	1	0.82	5,000	100-1700 <sup>a</sup>
F	1.70	—	—	—	—
G	0.87	1	0.67	350	100-4,300
H	1.05	10	1.20	5,200	100-8,600
I	2.80	1000	2.10	13,000	800-12,000
L	1.80	1000	1.95	25,000	800-12,000

<sup>a</sup> See Fig. 4.

When some crosslinks are introduced (in a very low degree, far below the gel point) there is a comparatively strong rise both of the stresses and of the relaxation times. In the meantime, a higher elasticity number is found. A similar effect is brought about by long branching. In general, stress relaxation phenomena are highly sensitive to crosslinking (even for a very low degree of crosslinking).

The accordance with a parabolic viscoelastic law, such as that expressed by eq. (10) has not proved successful or very significant, as is shown by the data of Table III. As happens occasionally in other fields of rheology (and in many branches of experimental physics) it may not be possible, in general, to find analytical functions (particularly simple ones) corresponding closely to experimental graphs such as our normalized stress relaxation curve. An analysis in a discrete series of simple analytical functions has already been made;<sup>2</sup> such an analysis has always some degree of arbitrariness.

At the present, we can state that the shapes of the normalized stress relaxation curves are highly sensitive to the general structural features considered here, namely average chain irregularity, polydispersity, slight degrees of crosslinking, and long branching. Therefore, such graphs can be practically used in order to investigate the polymer structure, at least in a qualitative and semiquantitative way.

Only a systematic investigation on a broad series of polymers having well known structural features can provide the basis for a quantitative evaluation of such features by means of stress relaxation measurements.

### References

1. Mussa, C., and V. Tablino, *J. Appl. Polymer Sci.*, **7**, 1391 (1963).
2. Mussa, C., and V. Tablino, *J. Appl. Polymer Sci.*, **6**, S21 (1962).
3. Mussa, C., *J. Appl. Polymer Sci.*, **7**, 1673 (1963).
4. Mussa, C., V. Tablino, and A. Nasini, *J. Appl. Polymer Sci.*, **5**, 574 (1961).

### Résumé

Après une revue des méthodes analytiques suggérées, on donne des exemples pratiques se rapportant à dix échantillons les polyéthylènes à haute et à basse pression, les polypropylènes atactiques et isotactiques et les caoutchoucs naturels. On voit la possibilité que les méthodes de mise en diagramme suggérées, ainsi que les grandeurs définies par cette analyse des données de la relaxation après la cessation d'un écoulement visqueux peuvent donner, dans le cas de ceux polymères, des renseignements qualitatifs et sémi-quantitatifs sur des caractéristiques structurelles, ainsi que la longueur moyenne de chaîne, la polydispersité, la régularité de chaîne, les ramifications longues et les réticulations.

### Zusammenfassung

Nach einer Übersicht vorgeschlagener analytischen Methoden, es wird beispielweise über zehn Mustern (Hoch- und Niederdruckpolyäthylenen, ataktischen und isotaktischen Polypropylenen und natürlicher Kautschuk) berichtet. Es zeigt sich die Möglichkeit dass die vorgeschlagenen Übertragungsmethoden der Spannungsrelaxationserscheinungen nach dem Aufhören eines stetigen Fließens, sowie die Grösse die durch eine solche Analyse bestimmt werden, Angabe über Struktureigenschaften leisten, sowie über durchschnittlichen Kettenlängen, Polymolekularität, Regelmässigkeit der Kettenstruktur, langen Verzweigungen und Vernetzungsgrad.

Received October 5, 1962